

Internal Report IASF-BO 540/2009

December 5, 2009

**NON-GAUSSIANITY TEST OF THE ILC WMAP 5YR MAP
THROUGH THE THREE POINT CORRELATION
FUNCTION IN THE EQUILATERAL CONFIGURATION**

C. BURIGANA¹, A. GRUPPUSO¹

¹*INAF-IASF Bologna, via P. Gobetti 101,
I-40129, Bologna, Italy*

December 5, 2009

**NON-GAUSSIANITY TEST OF THE ILC WMAP 5YR MAP
THROUGH THE THREE POINT CORRELATION
FUNCTION IN THE EQUILATERAL CONFIGURATION**

C. BURIGANA, A. GRUPPUSO

INAF-IASF Bologna, via P. Gobetti 101, I-40129, Bologna, Italy

SUMMARY- We report about the constraint on the non-Gaussianity parameter f_{NL} we obtain for the WMAP 5yr ILC map, through the computation of the three-point correlation function in the equilateral configuration. This has been possible performing 10^5 Monte-Carlo simulations of gaussian maps. The obtained constraint is consistent with those currently present in literature. Further work is needed to increase the resolution of the analysis in order to provide more stringent constraints.

1 Introduction

The anisotropy pattern of the Cosmic Microwave Background (CMB), obtained by Wilkinson Microwave Anisotropy Probe (WMAP) [1], and other astrophysical data sets provide a picture of the universe called Concordance Λ CDM model, a sort of Standard Model of Cosmology. According to this model, the universe is expanding as a Friedmann-Robertson-Walker (FRW) metric with a trivial flat spatial topology. Moreover the content of the universe is mainly split into Cold Dark Matter (CDM) for $\sim 25\%$, Dark Energy (DE) for $\sim 70\%$ and baryonic matter for $\sim 5\%$. Large scale structure (LSS) is assumed to be formed by gravitational collapse of an initially smooth distribution of adiabatic matter fluctuations, which were seeded by initial quantum fluctuations generated in a very early inflationary stage of the universe evolution. The simplest and commonly accepted model of Inflation, predicts that primordial fluctuations are Gaussian and independent. This means that primordial CMB fluctuations are Gaussian and isotropically distributed on the sky.

The aim of the present report is to test the WMAP 5yr ILC map versus these important predictions of the inflationary stage of the universe making use of the three-point correlation function defined in the equilateral configuration of the pixel space.

The report is organized as follows. In Section 2 we introduce the parameterization of the non-Gaussianity and its link with the well-known f_{NL} parameter. In Section 3 we define the three-point correlation function as an estimator of the level of non-Gaussianity present on a CMB map. Section 4 deals with the description of the performed simulations and with the results of our analysis concerning the WMAP 5yr ILC map. Discussions and conclusions are drawn in Section 5.

2 Non-Gaussianity model

We follow [2, 3] to parameterize the distance from a perfectly Gaussian model. Therefore we introduce implicitly the parameter a as follows

$$\delta T(\hat{n}) = \delta T_G(\hat{n}) + a \left(\delta T_G^2(\hat{n}) - \langle \delta T_G(\hat{n})^2 \rangle \right), \quad (2.1)$$

where $\delta T(\hat{n})$ is the total temperature fluctuation present in the pixel that is pointed by the normal vector \hat{n} . $\delta T_G(\hat{n})$ is the Gaussian temperature fluctuation in the same pixel and with the symbol $\langle \cdot \cdot \cdot \rangle$ we mean ensemble average. The parameter a is what has to be estimated in order to quantify the distance of $\delta T(\hat{n})$ from the pure Gaussian model $\delta T_G(\hat{n})$. Of course closer a to 0, closer $\delta T(\hat{n})$ to $\delta T_G(\hat{n})$.

In the large scale regime it is possible to use the Sachs-Wolfe expression:

$$\delta T(\hat{n}) = -\frac{T_0}{3} \phi(\hat{n}), \quad (2.2)$$

where T_0 is the CMB temperature and ϕ is the primordial gravitational potential, in order to connect the parameter a to f_{NL} more known and used in literature. After some algebra one finds

$$f_{NL} = -\frac{T_0}{3} a. \quad (2.3)$$

3 Three point correlation function

The estimator we want to consider in order to constraint a (and f_{NL}) is the three point correlation function C defined as follows:

$$C_3(\vec{\theta}) = \langle \delta T(\hat{n}_1) \delta T(\hat{n}_2) \delta T(\hat{n}_3) \rangle, \quad (3.1)$$

where $\vec{\theta} = (\theta_1, \theta_2, \theta_3)$ are the angles among the pixels pointed by the three normal vectors $\hat{n}_1, \hat{n}_2, \hat{n}_3$. Replacing equation (2.1) in equation (3.1) we have the following expansion

$$C_3(\vec{\theta}) = F_0(\vec{\theta}) + a F_1(\vec{\theta}) + a^2 F_2(\vec{\theta}) + a^3 F_3(\vec{\theta}), \quad (3.2)$$

with

$$F_0(\vec{\theta}) = \langle \delta T_G(\hat{n}_1) \delta T_G(\hat{n}_2) \delta T_G(\hat{n}_3) \rangle, \quad (3.3)$$

$$F_1(\vec{\theta}) = \langle \delta T_G(\hat{n}_1) \delta T_G(\hat{n}_2) \Delta T_G(\hat{n}_3) \rangle + \langle \delta T_G(\hat{n}_1) \Delta T_G(\hat{n}_2) \delta T_G(\hat{n}_3) \rangle + \quad (3.4)$$

$$\langle \Delta T_G(\hat{n}_1) \delta T_G(\hat{n}_2) \delta T_G(\hat{n}_3) \rangle, \quad (3.5)$$

$$F_2(\vec{\theta}) = \langle \delta T_G(\hat{n}_1) \Delta T_G(\hat{n}_2) \Delta T_G(\hat{n}_3) \rangle + \langle \Delta T_G(\hat{n}_1) \delta T_G(\hat{n}_2) \Delta T_G(\hat{n}_3) \rangle + \quad (3.6)$$

$$\langle \Delta T_G(\hat{n}_1) \Delta T_G(\hat{n}_2) \delta T_G(\hat{n}_3) \rangle, \quad (3.7)$$

$$F_3(\vec{\theta}) = \langle \Delta T_G(\hat{n}_1) \Delta T_G(\hat{n}_2) \Delta T_G(\hat{n}_3) \rangle, \quad (3.8)$$

where

$$\Delta T_G(\hat{n}) = \delta T_G^2(\hat{n}) - \langle \delta T_G(\hat{n})^2 \rangle. \quad (3.9)$$

An example of an algorithm aimed at the computation of the three point correlation function see [5].

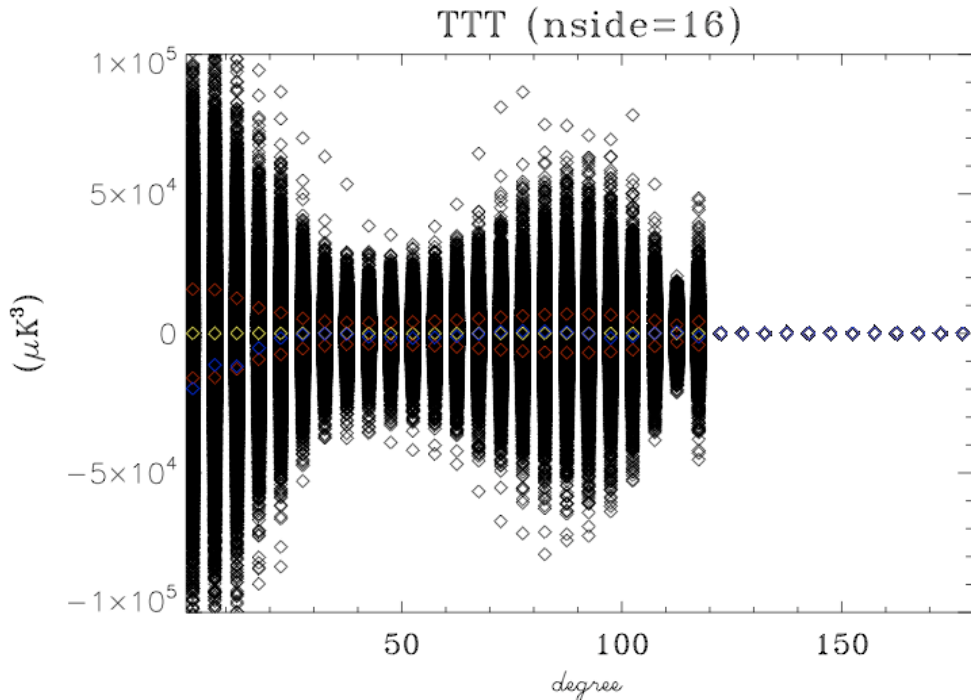


Figure 1: Three point correlation function in the equilateral configuration obtained from 10^5 realizations of Gaussian maps (signal plus noise, see also the text). Black diamonds: all the simulations. Red diamonds: 1σ level. Yellow diamonds: average of the simulations. Blue diamonds: WMAP 5yr ILC map. The angle θ is binned at 5° . At θ larger than 120° no correlation is possible by definition of the equilateral configuration. This is confirmed by our simulations. y-axis is in μK^3 and x-axis in angular degrees ($^\circ$).

4 Analysis and Results

In order to test the Gaussianity and therefore estimate a or f_{NL} of the WMAP 5yr ILC map we have performed 10^5 random map extractions where the signal map has been generated from the WMAP 5yr fiducial model and the noise map from the V band noise level (anisotropic white noise). These maps (signal + noise) have been used to build the functions F_0, F_1, F_2, F_3 where the equilateral configuration was specified (i.e. $\theta_1 = \theta_2 = \theta_3 = \theta$). Therefore C_3 (given by equation (3.1)) for the WMAP 5yr ILC map has been compared to C_3 obtained through Monte-Carlo simulations. The resolution used to make this analysis is $N_{side} = 16$, see Healpix [4]. This parameter corresponds to a number of pixels $N_{pix} = 3072$ (the relation between N_{side} and N_{pix} is given by $N_{pix} = 12 N_{side}^2$).

In Figure 1 we show the result of this comparison where C_3 for Monte-Carlo has been obtained by equation (3.1). The equilateral configuration prevents to have correlations for angles larger than 120° and this is recovered by our simulations (providing a consistency test for our f90 program). Figure 1 shows that the WMAP 5yr ILC map (blue diamonds) is always within 1σ level (red diamonds) except for the first binning. For “small” angles we note a trend for the WMAP 5yr ILC map going toward negative values of C_3 . Yellow diamonds stand for the average of the simulations (represented by black diamonds).

In Figure 2 we show the likelihood for a and f_{NL} obtained from the χ^2 analysis. In order to perform such an analysis we have considered the model (2.1). Therefore, in this case, the

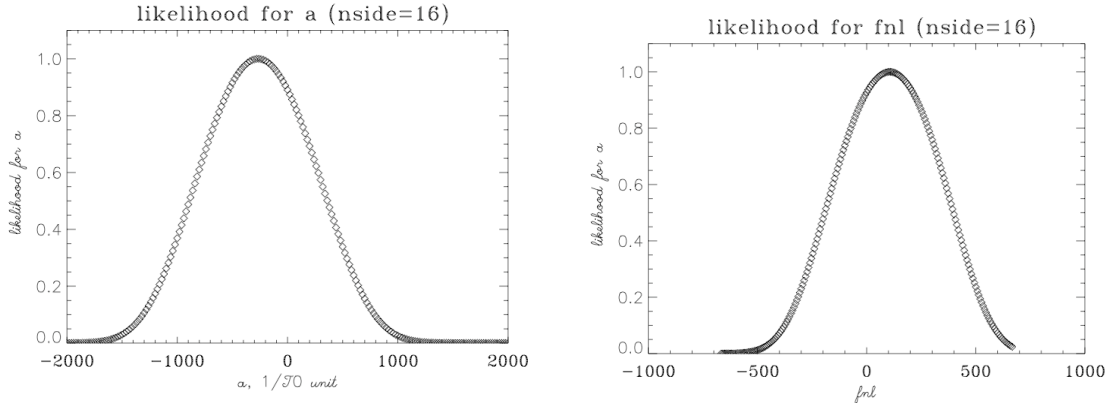


Figure 2: Left panel: likelihood for a . Right panel: likelihood for f_{NL} . In this case, in order to pass from a to f_{NL} we have neglected the contribution coming from the first binning (see equation 2.2 and 2.3).

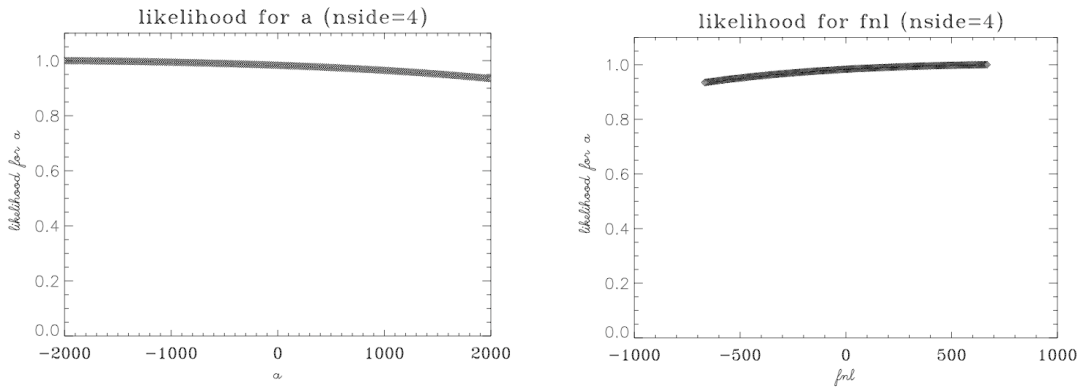


Figure 3: As Figure 2 but at $N_{side} = 4$.

C_3 obtained through Monte-Carlo simulations has been computed by the right hand side of equation (3.2), still in the equilateral configuration.

5 Discussion and Conclusion

It is very interesting to constraint the f_{NL} parameter, at the level we showed, even though the used resolution is not so high (i.e. $N_{side} = 16$). We are planning to parallelize the code to reach higher resolution to provide more stringent constraints to the non-Gaussian level of the WMAP 5yr ILC map. In order to understand the possible impact of the resolution on our analysis we plot in Figure 3 the constraints one obtains considering a lower resolution, corresponding to $N_{side} = 4$. Figure 3 shows that at very low resolution the capability to constraint the non-Gaussianity of the map is very low. Therefore we expect that increasing the resolution can provide more stringent constraint on f_{NL} . This argument can be extended up to the resolution where the noise does not become dominant.

Other configurations of the three point correlation function are possible extensions of the present analysis and deserve investigations.

References

- [1] C.L. Bennett et al., 2003, “First year Wilkinson Microwave Anisotropy Probe (WMAP) Observations: preliminary maps and basic results”. *ApJS*, 148, 1
- [2] P. Vielva and J. L. Sanz, “Analysis of non-Gaussian CMB maps based on the N-pdf. Application to WMAP data,” arXiv:0812.1756 [astro-ph].
- [3] P. Vielva and J. L. Sanz, “Constraints on f_{nl} and g_{nl} from the analysis of the N-pdf of the CMB large scale anisotropies,” arXiv:0910.3196 [astro-ph.CO].
- [4] K.M. Gorski, E. Hivon, A.J. Banday, B.D. Wandelt, F.K. Hansen, M. Reinecke, and M. Bartelmann, HEALPix: A Framework for High-resolution Discretization and Fast Analysis of Data Distributed on the Sphere, *Ap.J.*, 622, 759-771, 2005.
- [5] H. K. Eriksen, A. J. Banday, K. M. Gorski and P. B. Lilje, *Astrophys. J.* **622**, 58 (2005) [arXiv:astro-ph/0407271].